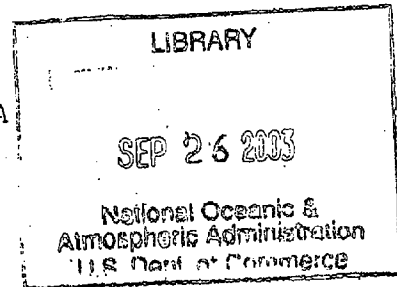


Supplement to Meteorology 201 A

Issued October 1953



RAREBOOK
QC
880.4
.A8
B56
1953

The Problem of Cyclogenesis From Helmholtz
Time to the Present

By J. Bjerknes

University of California, Los Angeles

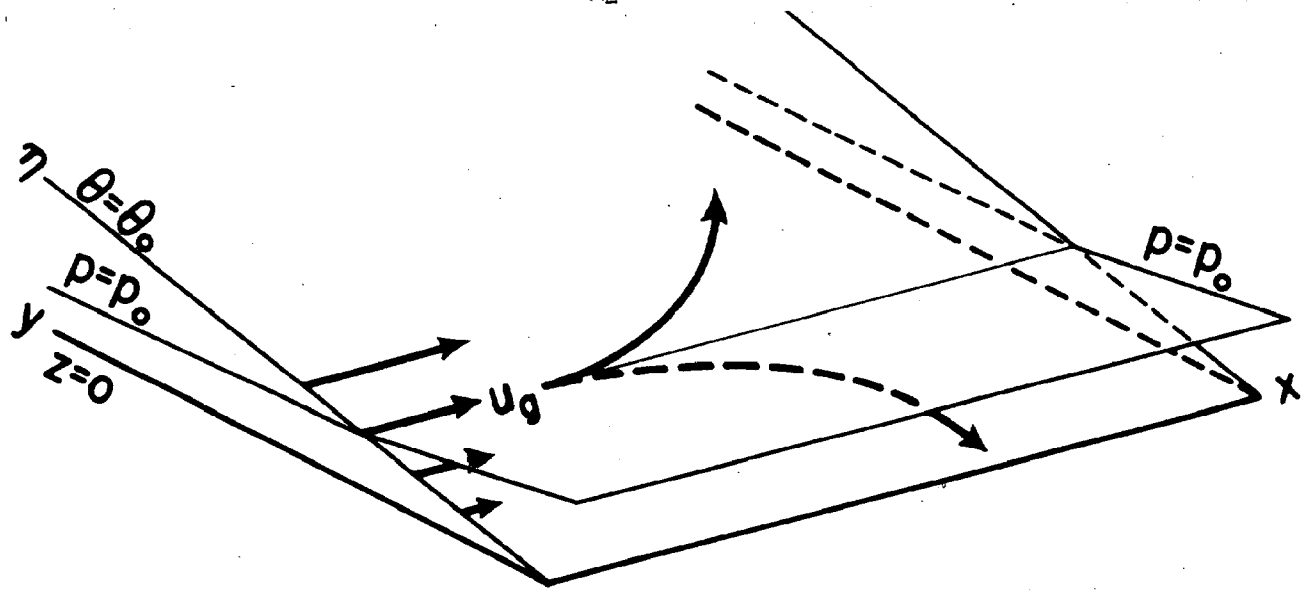
It was in 1868 that Helmholtz presented the principle of "dynamic instability" which contains the key to the understanding of frontal cyclogenesis. I will here re-state the principle in a simplified form and try to adapt it for the use in synoptic meteorology.

The upper part of Fig. 1 shows a model of the baroclinic westerlies with an isentropic surface rising northwards from its intersection with the ground, which is taken as the x-axis. The y-axis points horizontally northwards and another axis, denoted η , is pointing northwards along the upslope of the isentropic surface. The air current flows along the x-direction, but it is assumed that individual sample particles may oscillate (without friction) in the $x\eta$ -plane. While keeping to the isentropic surface, the particles automatically adopt the temperature of the environment at each new location, and are not subject to any buoyancy forces. The oscillation of the sample particle is controlled by the joint action of the pressure gradient and the Coriolis force. The acceleration of the particle in the η -direction under that joint influence is

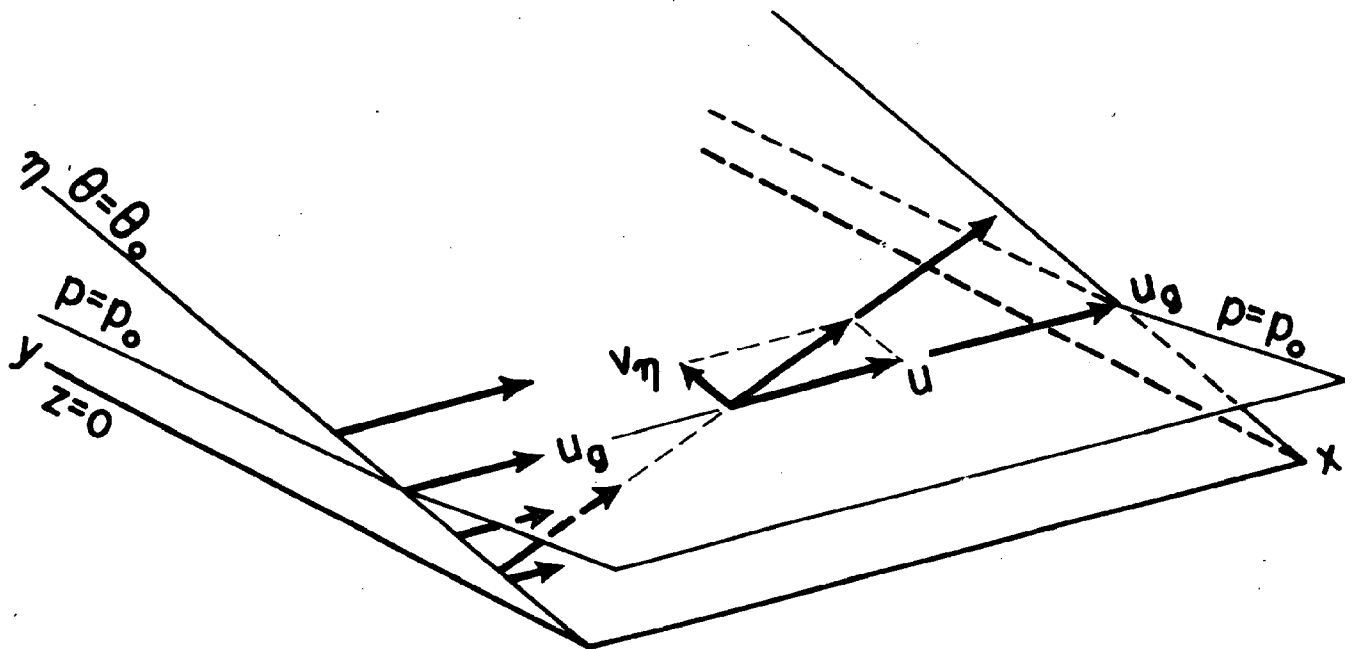
$$(1) \quad \frac{d^2 \eta}{dt^2} = -2\Omega_2 (u - u_g),$$

where $2\Omega_2 = 2\Omega \sin \phi$ is the Coriolis factor and u_g is the geostrophic wind. The x-component of the acceleration of a perturbed particle is

$$(2) \quad \frac{du}{dt} = 2\Omega_2 v_\eta,$$



$$\frac{\partial u_g}{\partial \eta} > 2\Omega \sin \varphi$$



$$v_\eta = u \frac{\partial u_g}{\partial x} / (2\Omega \sin \varphi - \frac{\partial u_g}{\partial \eta})$$

Fig. 1. Upper part: Model of baroclinic straight westerlies. Particles are freed from geostrophic control in the case of "dynamic instability" defined by $\frac{\partial u_g}{\partial \eta} > 2\Omega \sin \varphi$.

Lower part: Model of baroclinic, confluent westerlies with weak dynamic stability. Stable isentropic upgliding is possible at the rate

$$v_\eta = u \frac{\partial u_g}{\partial x} / (2\Omega \sin \varphi - \frac{\partial u_g}{\partial \eta}).$$

and the change of environmental geostrophic wind seen by an observer following the travelling particle

$$(3) \quad \frac{du_g}{dt} = v_\eta \frac{\partial u_g}{\partial \eta}$$

If $\left| \frac{du_g}{dt} \right| > \left| \frac{du_p}{dt} \right|$, that is $\frac{\partial u_g}{\partial \eta} > 2\Omega_2$, the particle would acquire according to (1), an acceleration component in η -direction of the same sign as the initial perturbation velocity v_η , hence the current would be dynamically unstable in the sense of Helmholtz. The relationships

$$(4) \quad \frac{\partial u_g}{\partial \eta} \begin{matrix} \geq \\ = \\ < \end{matrix} 2\Omega_2$$

define, respectively the unstable, the indifferent, and the stable case of inertial oscillations in the isentropic surface.

The possibility of checking the Helmholtz instability criterion under real atmospheric conditions has only recently materialized with the creation of good networks of upper air stations. Fig. 2 shows one such evaluation of the quantity $2\Omega_2 - \frac{\partial u_g}{\partial \eta}$ on the basis of Palmén & Newton's average cross-section through slow moving winter time fronts over the eastern United States. The most unstable region, by the Helmholtz definition, is just south of the jet stream high above the frontal surface. The air at the frontal surface itself is not dynamically unstable, but, relatively less stable than the air masses on either side of it. The main reason for the diminished stability at the front is the fact that upgliding inside the frontal cloud takes place moist-adiabatically and hence at a greater angle with the horizontal in the profile, which in turn results

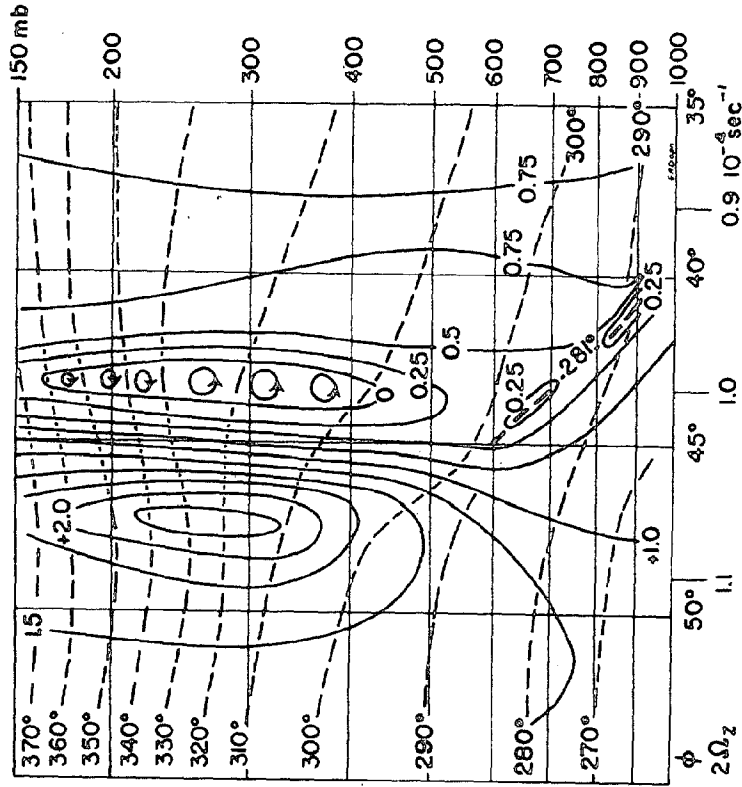
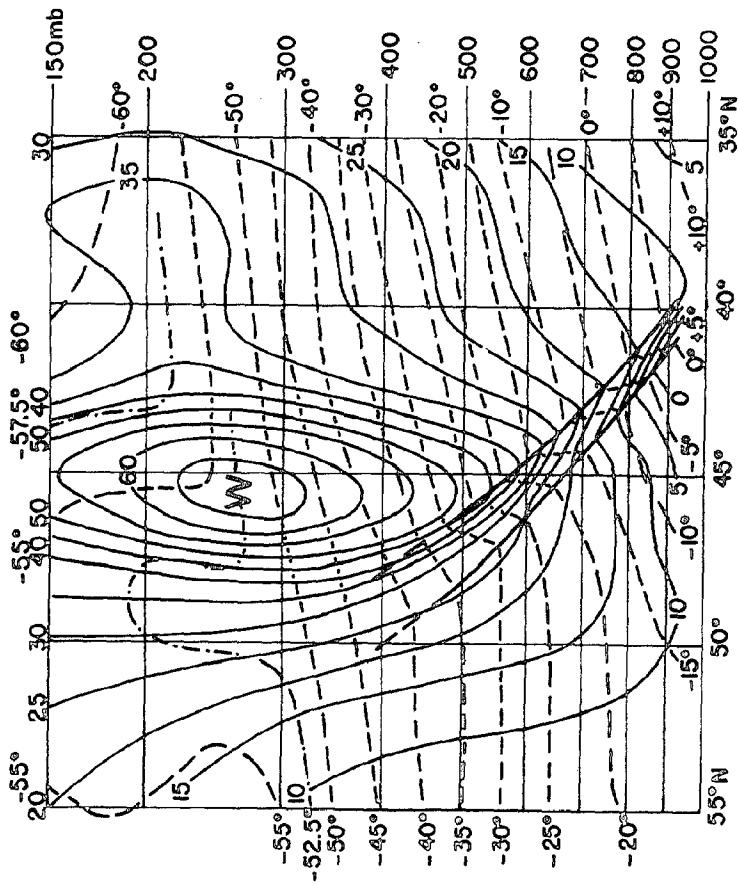


Fig. 2. Meridional profiles through a model of straight westerlies with quasi-stationary polar front (Palmen and Newton 1948). Left: Dashed lines show isotherms (centigrade) and solid lines isotachs ($m\ sec^{-1}$) of zonal geostrophic wind. Right: Dashed lines show the field of dry-isentropes (degrees absolute) and the saturation isentropes of 281° in the frontal zone. Solid lines represent the quantity $(2\sigma \sin \phi - \partial \bar{u}_g / \partial \eta)$ in units of $10^{-4}\ sec^{-1}$. Dynamic instability is barely reached in a zone south of the jet stream.

in greater $\frac{\partial \mu_g}{\partial \eta}$ values. The Margules equilibrium at a front is therefore more easily disturbed by an impulse upward than downward along the isentropes of the frontal zone. An upslope impulse imparted to the saturated air on a quasistationary front can be considered as the most likely initiation of frontal cyclogenesis.

From the checking in Fig. 2, and in many other individual frontal situations, it appears that dynamic instability as defined in (4) is too infrequent an occurrence to be responsible for the very frequently observed frontal cyclogenesis. But a slight change in the model from parallel to confluent westerlies improves the chances of frontal cyclogenesis greatly. That case is illustrated in the lower part of Fig. 1. The sample particle in that model experiences a change in the environmental geostrophic wind both by its displacement in x- and η -direction

$$(5) \quad \frac{d\mu_g}{dt} = u \frac{\partial \mu_g}{\partial x} + v_\eta \frac{\partial \mu_g}{\partial \eta}$$

and the case of $\frac{d\mu_g}{dt} = 0$ will occur when $\frac{dv_\eta}{dt} = \frac{d\mu_g}{dt}$, or (approximately)

$$(6) \quad 2\Omega_2 v_\eta = u \frac{\partial \mu_g}{\partial x} + v_\eta \frac{\partial \mu_g}{\partial \eta}$$

That condition of un-accelerated cross-isobaric flow at the rate v_η occurs when v_η has the adjusted value obtained from (6)

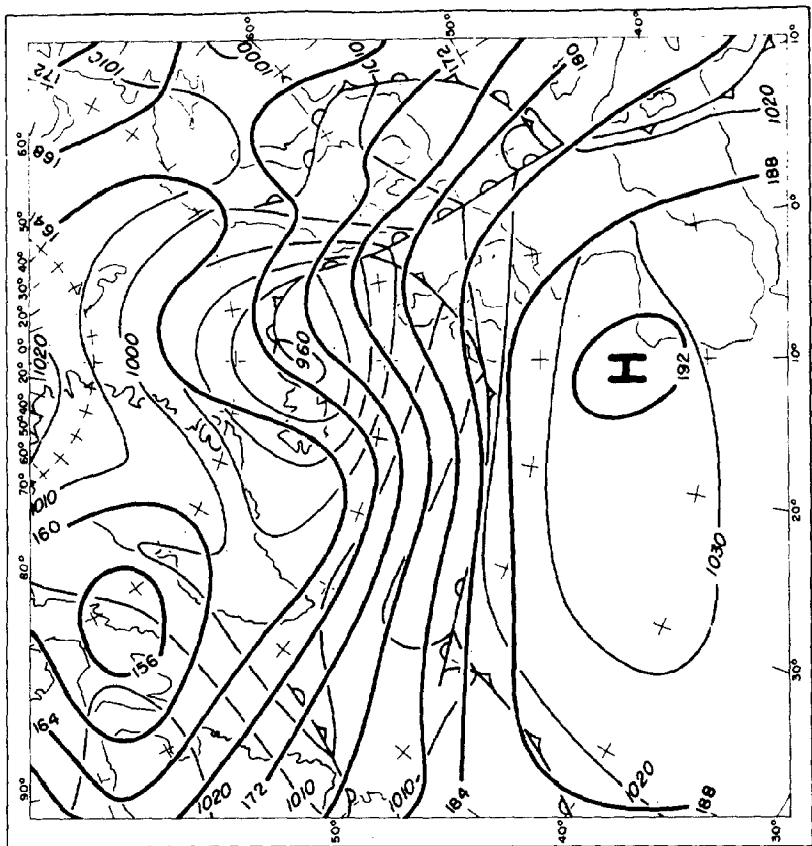
$$(7) \quad v_\eta = \frac{u \frac{\partial \mu_g}{\partial x}}{2\Omega_2 - \frac{\partial \mu_g}{\partial \eta}}$$

In the normal case $2\Omega_2 > \frac{\partial \mu_g}{\partial \eta}$ the upgliding component v_η will oscillate about its adjusted value in (7). That upgliding is favored by great values of a "confluence parameter" $u \frac{\partial \mu_g}{\partial x}$ and by small values of the "stability parameter" $2\Omega_2 - \frac{\partial \mu_g}{\partial \eta}$, which is the same one that measures the dynamical

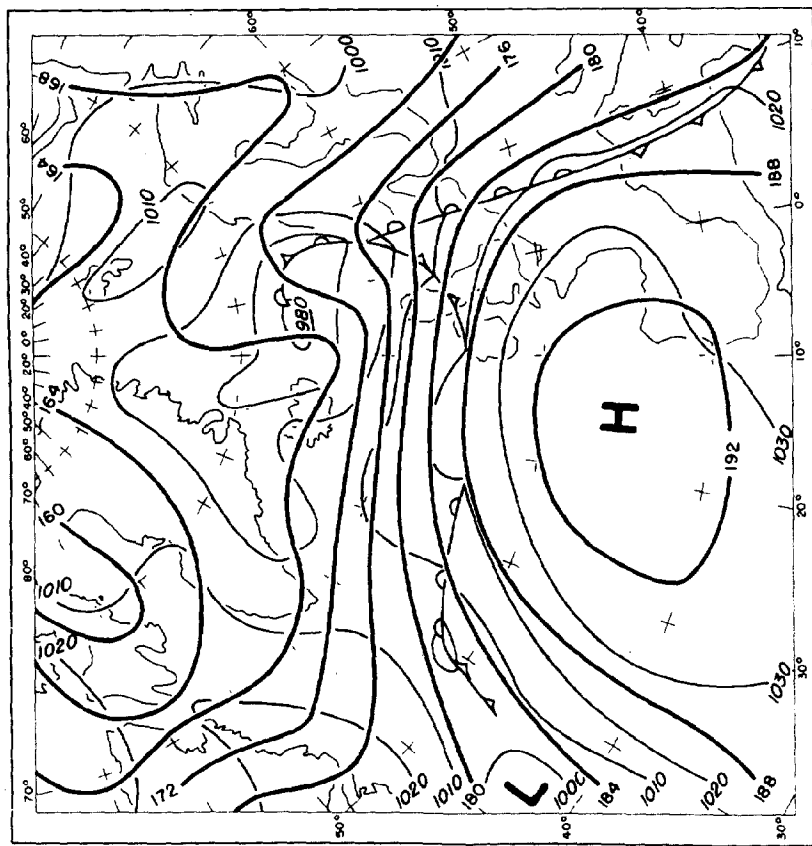
stability in the sense of Helmholtz.

It is the experience of this writer that equation (7) is a good guide in indicating the location and probable intensity of impending cyclogenesis. The maps in Fig. 3 may serve as a typical illustration. For each date, January 16 and 17, 1949, the 500 mb map has been superposed on the surface map. The young cyclone which was over the mid-Atlantic on the 16th and traveled to a point east of Iceland the next day, while deepening from 1000 mb to 960 mb, had the ideal growth conditions defined by (7). The sharp pre-existing front is a sign of lessened dynamic stability, and the confluence of the upper current over the region of cyclogenesis is clearly evident from the 500 mb map. Similar conditions, although not quite as pronounced, favored the deepening of the next young cyclone over the mid-Atlantic on the 17th.

The mechanism by which the cyclone intensification is tied to the upgliding can be demonstrated through vorticity considerations: the stronger the upgliding the more convergence at the ground to feed the upcurrent and the more cyclonic vorticity must result from the convergence. But another question remains to be answered: with all the convergence in low layers into the central column of the cyclone how can the pressure be falling there during the deepening process? The answer is of course known to be: upper level divergence overcompensates the low level convergence. That upper level divergence has been shown by Holmboe (1944) to be an inherent feature of the forward half of upper air troughs up beyond a "level of non-divergence" as illustrated schematically in Fig. 4. If



17 JANUARY 1949



16 JANUARY 1949

Fig. 3. 500 mb topography superposed on sea level map on two successive days. On both days frontal cyclogenesis takes place in mid-Atlantic under confluent upper flow. Fully developed occluded cyclones E of Iceland both are associated with diffluent upper troughs. The phase lag of the upper troughs relative to the surface centers is real, but is exaggerated by the time lag of the surface map (9 hours).

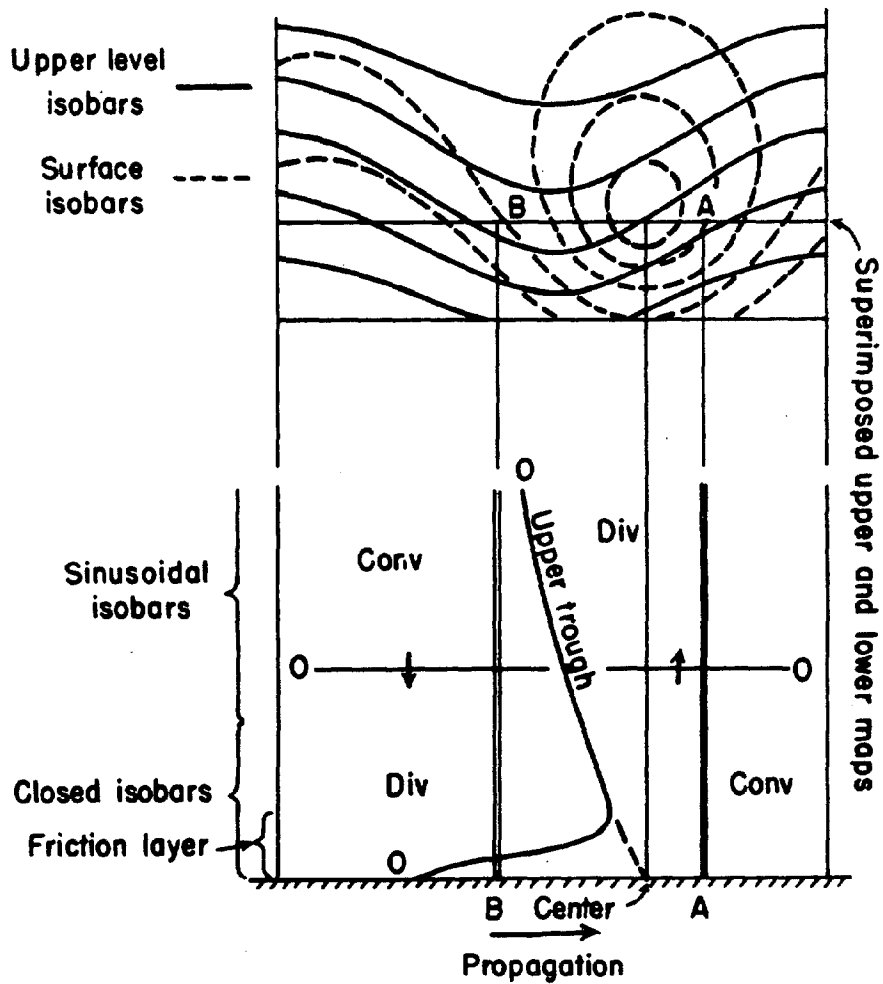


Fig. 4. Model of cyclone with closed isobars in low levels and a trough in upper levels lagging behind the surface center (Holmboe and Bjerknes 1944). Pre-trough upper divergence overlies the surface center.

there is a phase difference between the surface center and the upper level trough, in the sense that the upper trough lags behind, the upper divergence will be operating vertically above the low level convergence in the cyclone center. This does not yet assure the deepening; many cyclones with the right lag of the upper trough do not deepen, because the pre-trough upper divergence is not strong enough to overcompensate the low level convergence.

One important point in the forecasting of the formation of deep storm centers is therefore to decide early whether the upper air divergence will have optimum chances of development. A partial answer to that question is: available from the theory of the waves in the westerlies: the stronger the upper winds streaming through the upper trough, the stronger the pre-trough upper divergence; in other words, the more strongly baroclinic the initial situation is, the greater the chance for deepening. In winter north of 55°N , when the baroclinicity continues in the same sense in the known part of the stratosphere as in the troposphere, the strong westerlies extend higher up than in other latitudes and seasons, and presumably provide for the strongest upper divergence effects available above any extra-tropical cyclones.

Another typical feature associated with the maximum possible upper air divergence can be seen in Fig. 3. The young cyclone was born the 16th under the upper divergence east of a pre-existing upper trough in SSW-NNE orientation, but the new upper trough that develops together with the deepening cyclone center takes on the SSE-NNW orientation seen on the 17th.

(The corresponding upper trough behind the preceding Iceland cyclone on the 16th shows an even more obvious SE-NW orientation).

The reason for the SE-NW orientation must be sought in the initial meridional shear $\frac{\partial u}{\partial y}$, north of the latitude of maximum upper westerlies. Waves superimposed on a current with that kind of shear move faster in the south than in the north and eventually attain the SE-NW orientation.

SE-NW troughs in the westerlies are by kinematic necessity "diffluent troughs", that is, the isobars and streamlines combine the cyclonic curvature in the trough with a spreading downwind. Particles overtaking such a trough must undergo retardation, and therefore must move with a component towards high pressure while making the cyclonic turn. Movement towards high pressure in a cyclonic bend of a current involves horizontal divergence, and we are thus led to state that in diffluent troughs the zero line between pre-trough divergence and post-trough convergence must lag behind the trough line. That kind of a trough, extending through all layers above the level of non-divergence, should contribute strongly to the general deepening of the cyclone. It is probably a matter of dynamic significance that both of the two full-grown cyclones in Fig. 3, and most other big cyclones, are associated with diffluent upper troughs, undoubtedly a more efficient flow pattern for removing air aloft than that of the symmetric upper wave in Fig. 4.

Summing up the characteristics of frontal cyclogenesis, we see two main processes involved, (1) the isentropic upgliding (and low level in-flow) at a front under a confluent upper current whose dynamic stability

is weak, and (2) the removal of air above the cyclone through the divergence in, and ahead of, the upper diffluent trough which forms together with the frontal cyclone, and whose structure and orientation (SE-NW) is due to the cyclonic shear north of the jet stream.

Literature References

- Helmholtz, H. von, "Über atmosphärische Bewegungen" Meteorologische Zeitschrift, 5: 329-340 (1888).
- Holmboe, J. and Bjerknes J., "On the Theory of Cyclones". Journal of Meteorology, 1: 1-22 (1944).
- Palmen, E. and Newton, C.W., "A Study of the Mean Wind and Temperature Distribution in the Vicinity of the Polar Front in Winter". Journal of Meteorology, 5: 220-226 (1948).